Title
TESTING THE PERFORMANCE OF SCINTILLATION CAMERAS

Author
Anger, H.O.

Publication Date
1973-05-01

LBL-2027 c.1
UC-37 Instruments
TID-4500 (59th Ed.)

TESTING THE PERFORMANCE OF SCINTILLATION CAMERAS

H. O. Anger
DONNER LABORATORY

May 1973

Prepared for the U.S. Atomic Energy Commission under Contract W-7405-ENG-48

DISCLAIMER

LBL-2027

Testing the Performance of Scintillation Cameras

H. O. Anger

May, 1973

Donner Laboratory
and
Lawrence Berkeley Laboratory
University of California
Berkeley, California 94720

AEC Contract No. W-7405-eng-48

Introduction

A method is described for testing the inherent resolution of scintillation cameras as a function of count rate. It involves the use of a new test pattern with hexagonal arrays of holes and a "point" source of Technetium-99m at a distance covered by a series of lead absorbers to change the effective source strength through a series of values. The new test pattern is believed to be superior to the bar patterns now in use.

The sensitivity of the image detector can be determined as a function of count rate at the same time. A simple method is also described that demonstrates whether the setting of the pulse-height selector is critical with regard to the field uniformity obtained.

This report has been written to describe the test procedure and to show that by its use significant differences in the performance of scintillation cameras can be demonstrated. It is not intended to be a comprehensive report on the relative performance of different commercial instruments.

Apparatus and Method

The test set-up is shown in Fig. 1. The collimator is removed from the scintillation camera and the test pattern is positioned as close to the scintillator as possible. About 100 millicuries of Technetium-99m in a plastic vial is placed 100 cm away on the central axis. A plastic vial is used because glass containers have appreciable gamma-ray absorption. Lead absorbers are placed over the source to decrease its apparent strength through a 100 to 1 range of values as the test progresses.

A drawing of one sector of the test pattern is shown in Fig. 2. It consists of a lead plate with holes drilled in a hexagonal array. The complete test pattern consists of six sectors having holes with center-to-center distances given in the Table. In each case, the hole diameter is one-fourth of the center-to-center distance. Maximum hole spacing was 20 mm and minimum was 8 mm in the pattern used for the tests reported here.

In the author's opinion, this pattern is better than the widely-used bar patterns for demonstrating inherent resolution, because there is a sharper cut-off between resolved and non-resolved spacings. The resulting images of the holes are better than lines for demonstrating astigmatism, which is a blurring of the spots in one direction only. Also the wide dark bands are useful for detecting a background of randomly placed dots which some scintillation cameras exhibit at high counting rates.

A series of separately calibrated sources of different strengths can be used for the tests described here, but the author has found it more convenient to use a single strong source and reduce the intensity with lead absorbers.

The absorption of Technetium-99m gamma rays by lead foils has been checked experimentally and found to agree closely with that given from interpolation of the data by Grodstein (1). For the convenience of those who may want to run similar tests, the calculated absorption factor for lead foils is plotted in Fig. 9.

The volume of liquid in a 100 millicurie source is usually large enough that appreciable absorption occurs in the source itself. A correction can be made by measuring the height of the liquid and obtaining a self absorption factor from the curve in Fig. 10. The equivalent source strength is equal to the actual number of millicuries in the source times the product of the lead foil absorption factor and the self absorption factor.

In the tests reported here, either the assay of the commercial supplier of the Technetium was used, or a part of the solution was measured with a dose calibration instrument. The accuracy of the sensitivity measurements are therefore limited by the accuracy of this calibration.

Resolution Tests

To run the inherent resolution tests shown in Figs. 3 through 8, the test pattern and Technetium source were arranged as shown in Fig. 1, the source was covered with five .014 inch lead foils, and the PHS window was adjusted for normal operation.

A scintiphoto with one million counts was taken and the required time was recorded. Then one of the lead foils was removed from the source and another scintiphoto with one million dots was taken. Again, the time was recorded. The process was repeated until the scintillation camera jammed or until no foils were left on the source.

Sensitivity Tests

From the time required to register one million dots, the counting rate is calculated, and from the equivalent source strength in millicuries, the camera sensitivity in terms of counts per second per millicurie is calculated. Both are shown below the respective scintiphotos in Figs. 3 through 8.

The calculated geometric counting efficiency, including a small amount of gamma-ray leakage through the lead test pattern, is such that one millicurie of Technetium-99m in the source should result in a count rate of about 10,000 per second when the source strength is low and dead time losses are small. A ± 10% variation from this rate is probably not significant because of errors in calibration of the source, variations in width of the photopeak and setting the PHS window, etc. The sensitivity decreases because of dead time losses as the counting rate goes up. The loss can be checked against that expected from the manufacturer's dead time specification.

Field Uniformity Tests

To check the field uniformity the resolution pattern was removed, the source was covered with enough lead foils to reduce the count rate to about 10,000 counts per second, and flood pictures were taken. First a scintiphoto was taken with the PHS window centered on the photopeak. The count rate was noted, and then the PHS window was purposely displaced far enough toward the lower portion of the photopeak to reduce the counting rate to one half of normal and another flood picture was taken. Then the PHS window was displaced far enough to the upper portion of the photopeak to obtain the same reduced count rate and a third flood picture was taken. Each picture had one million dots. The purpose of displacing the PHS window as described here is to show in an exaggerated way how the field uniformity is affected by misadjustment of the PHS window. The results are shown in Figs. 3 through 8.

Interpreting the Results

It is left for the reader to interpret the results as shown in Figs. 3 through 8. At the risk of stating the obvious and being repetitive, the following points should be observed:

1. Inherent resolution at low counting rates.

2. Degradation of resolution as counting rate is increased.
3. Astigmatism (can indicate misadjustment of ratio circuits).
4. Stray dots in normally black areas.
5. Spatial distortion.
6. Change of CRT intensity with count rate.
7. Field size (is less than pattern diameter if part of the pattern is not seen in scintiphotos).
8. Sensitivity (see text for discussion).
9. Field uniformity with normal PHS window.
10. Reduction in field uniformity when PHS window is misadjusted.

It should be pointed out that ordinary clinical tests do not require the highest count rates encountered in the tests reported here. The usual high-sensitivity, low-energy collimator passes only about one-half as many gamma rays per millicurie as the test arrangement.

Also, the overall resolution of a system does not depend upon inherent resolution alone. It depends partly upon collimator characteristics as discussed in reference (2).

It should be stressed again that the tests shown here are very limited because, with one exception, only one unit of a given commercial model of scintillation camera was tested. Although all the instruments were in clinical use, additional tests would be required to show whether they were in top operating condition and whether the performance reported here is typical of others with the same model designation.

References

Grodstein, G. W., X-ray attentuation coefficients from 10 kev to 100 Mev. National Bureau of Standards Circular 583, p. 45, 1957.

2. Anger, H. O., Radioisotope Cameras. In "Instrumentation in Nuclear Medicine, Vol. 1", pp. 514-527, ed. by G. W. Hine, Academic Press, New York.

Acknowledgments

This work was supported by the U.S. Atomic Energy Commission. A trip to Columbus, Ohio, to test the Ohio Nuclear and Picker Scintillation cameras was supported by the Nuclear Medicine Department of the Ohio State University.

Thanks are extended to Mr. Jerome Dare, Ohio State University, Columbus, Ohio; Dr. Paul Weber, Kaiser Hospitals, Oakland, California; Dr. William Wedemyer, Herrick Hospital, Berkeley, California; and to Mr. Robert Haines, Sacramento Medical Center, Sacramento, California, for permission and aid in testing their scintillation cameras.

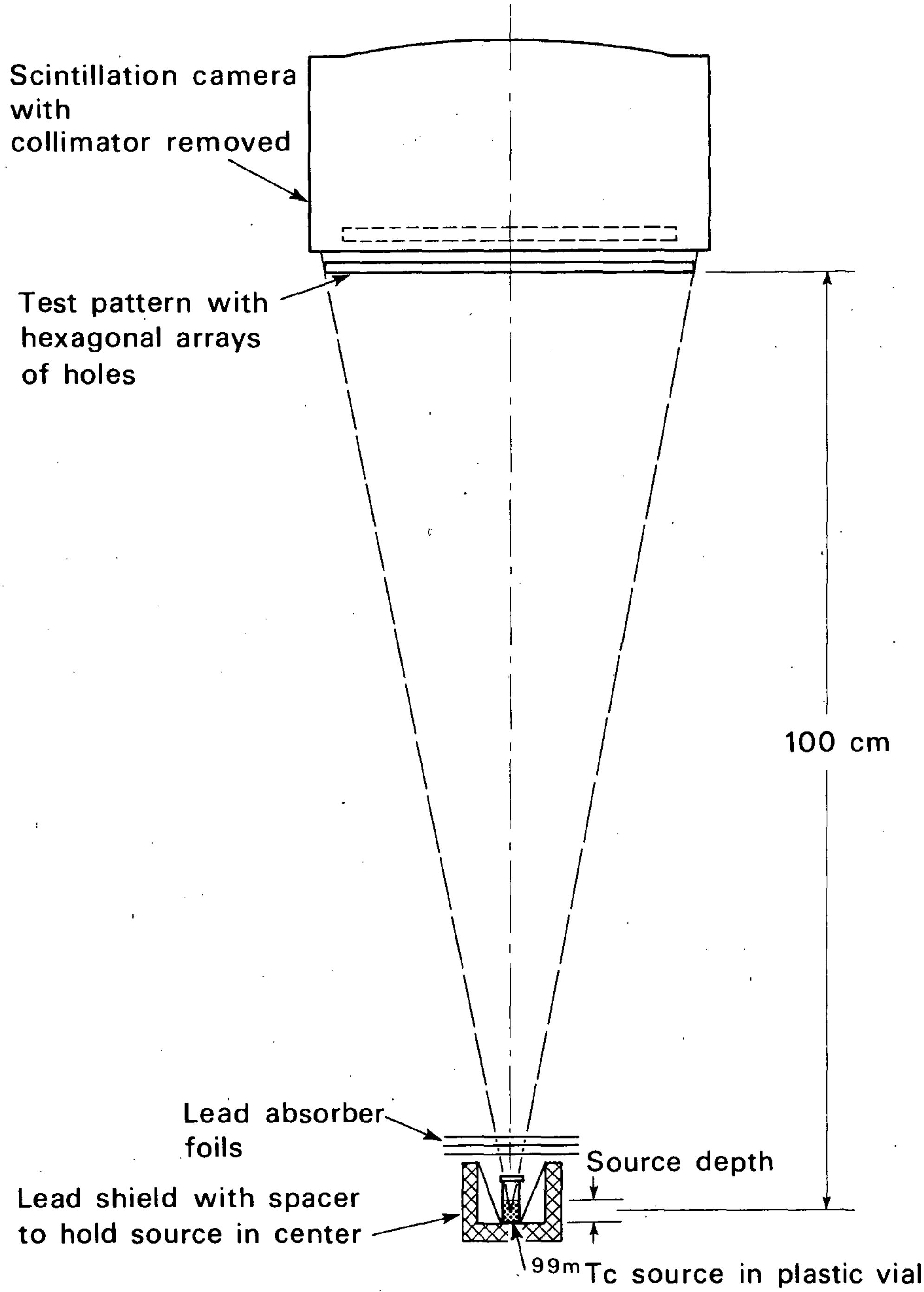

DBL 736-5194

Fig. 1 Schematic drawing of test arrangement for demonstrating inherent resolution of scintillation camera image detectors at various counting rates.

A (Hole spacing center to center)	$\frac{A}{4}$ (Hole diam.)	Total no. of holes in sector
20 mm	5 mm	30
16	4	48
14	3.5	58
12	3	71
10	2.5	108
8	2	157

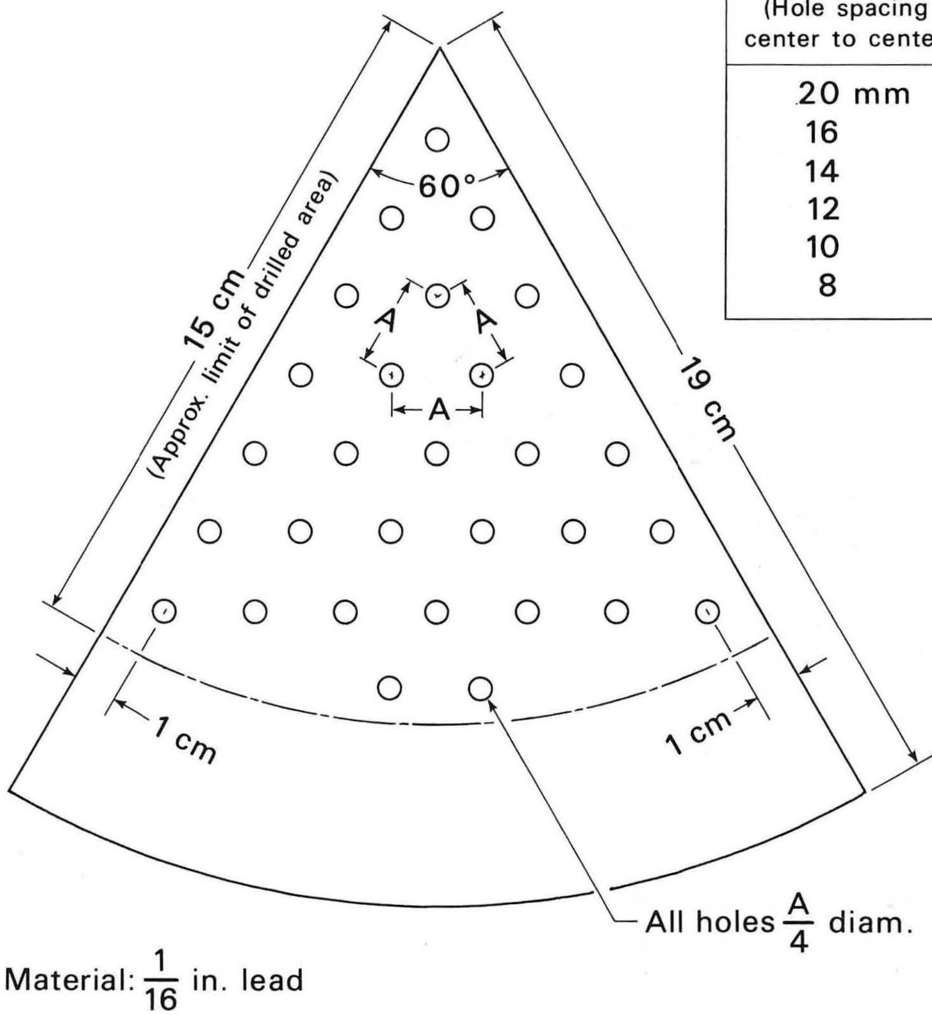

DBL 736-5195

Fig. 2 Section of test pattern. The full pattern consists of six sections with hole spacings and diameters given in the table.

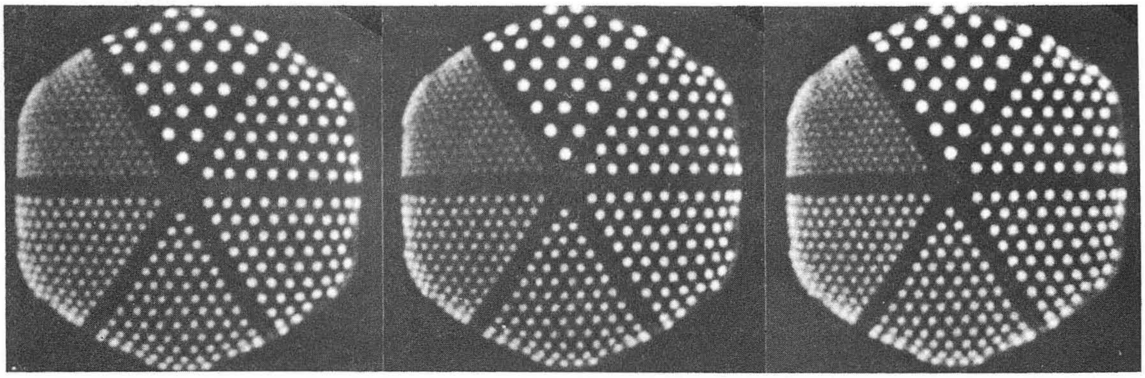

A. 0.85 mCi Equiv.
9,200 c/s
10,800 c/s/mCi

B. 2.1 mCi Equiv.
20,400 c/s
9,600 c/s/mCi

C. 5.4 mCi Equiv.
42,000 c/s
7,700 c/s/mCi

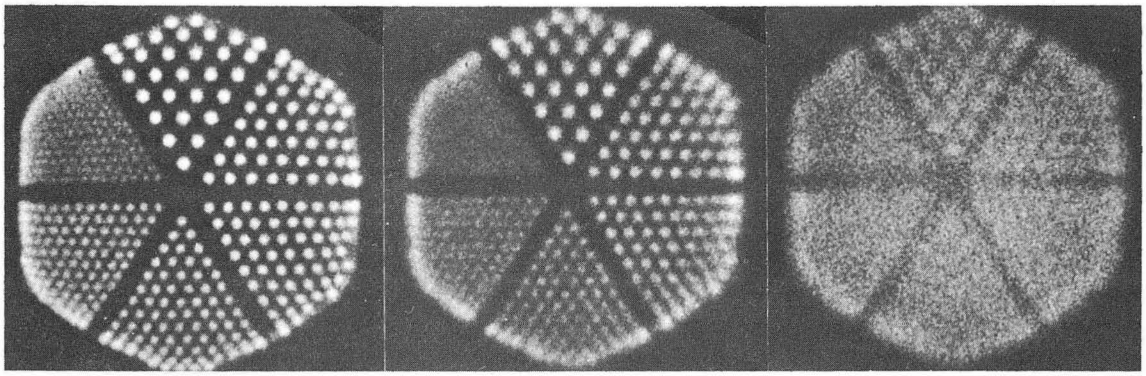

D. 14 mCi Equiv.
62,000 c/s
4,500 c/s/mCi

E. 35 mCi Equiv.
47,000 c/s
1,360 c/s/mCi

F. 88 mCi Equiv.
16,400 c/s
185 c/s/mCi

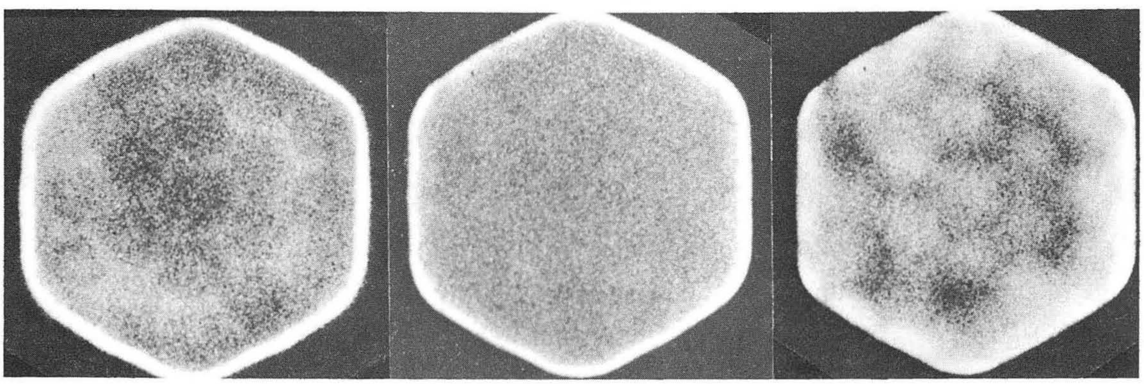

G. Flood with PHS window on lower portion of photopeak

H. Flood with PHS window centered on photopeak

I. Flood with PHS window on upper upper portion of photopeak

Fig. 3 Ohio-Nuclear series 100 radioisotope camera installed March, 1973 at the Ohio State University.

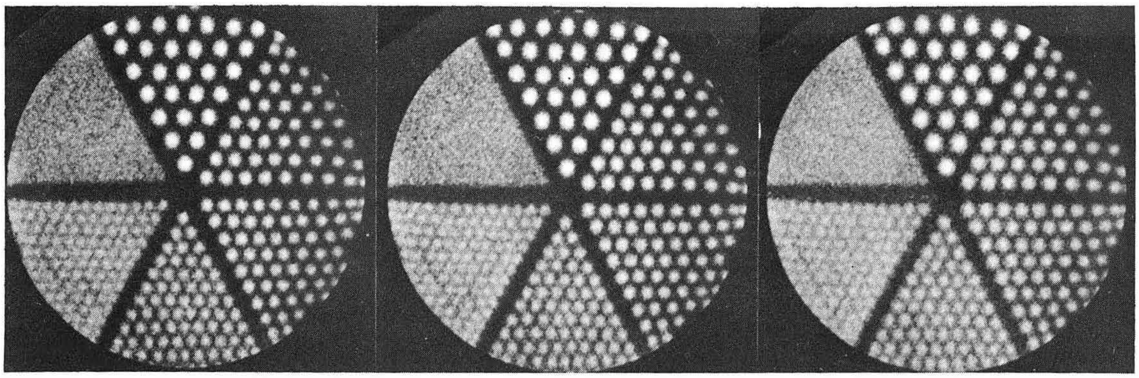

A. 1.1 mCi Equiv.
7,700 c/s
7,200 c/s/mCi

B. 2.7 mCi Equiv.
13,000 c/s
4,800 c/s/mCi

C. 6.9 mCi Equiv.
17,000 c/s
2,500 c/s/mCi

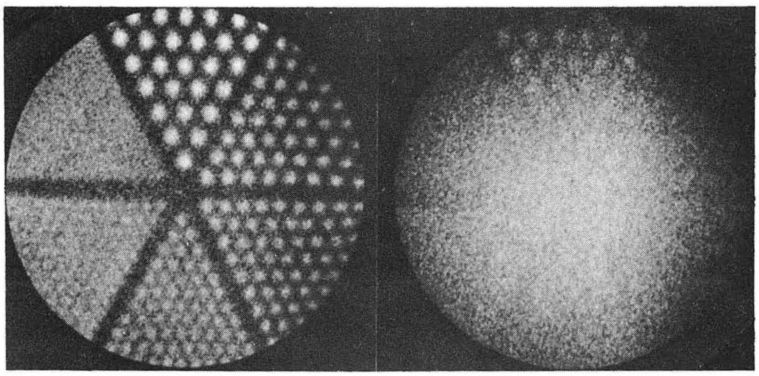

D. 17 mC Equiv.
14,000 c/s
780 c/s/mCi

E. 45 mC Equiv.
2,500 c/s
55 c/s/mCi

F.

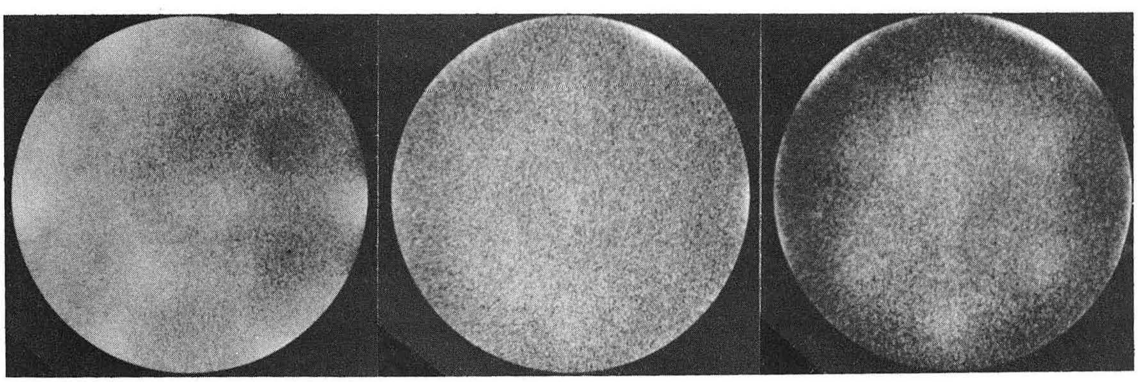

G. Flood with PHS window on lower portion of photopeak

H. Flood with PHS window centered

I. Flood with PHS window on upper portion of photopeak

Fig. 4 Picker DynaCamera 2C installed September, 1972 at Ohio State University.

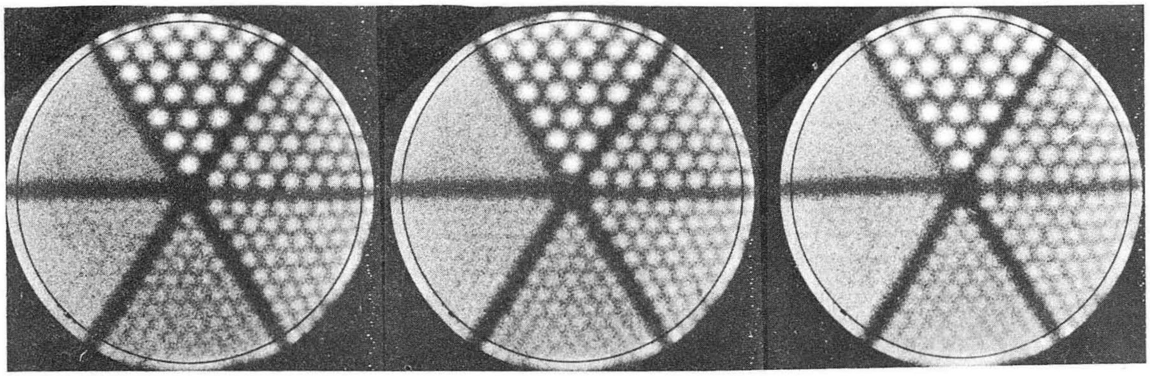

A. 0.73 mCi Equiv.
7,100 c/s
9,700 c/s/mCi

B. 1.8 mCi Equiv.
16,600 c/s
9,000 c/s/mCi

C. 4.7 mCi Equiv.
31,700 c/s
6,800 c/s/mCi

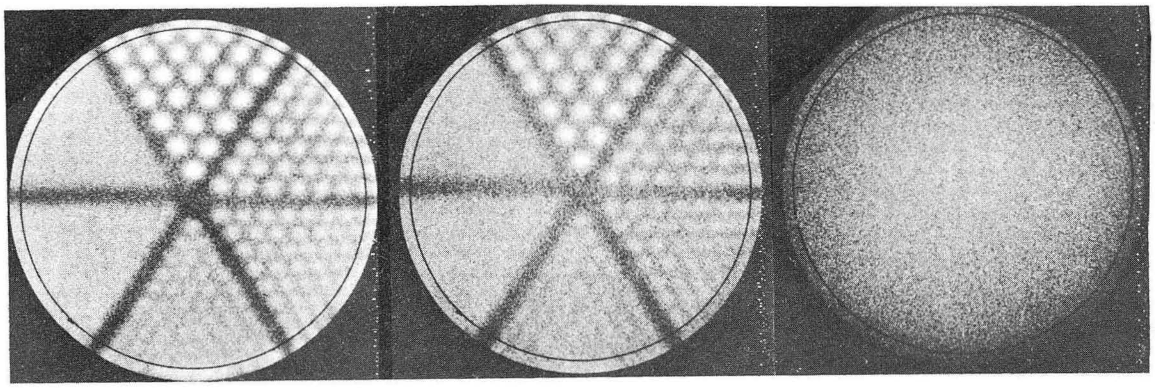

D. 11.8 mCi Equiv.
60,400 c/s
5,100 c/s/mCi

E. 30 mCi Equiv.
66,600 c/s
2,230 c/s/mCi

F. 76 mCi Equiv.
32,500 c/s
430 c/s/mCi

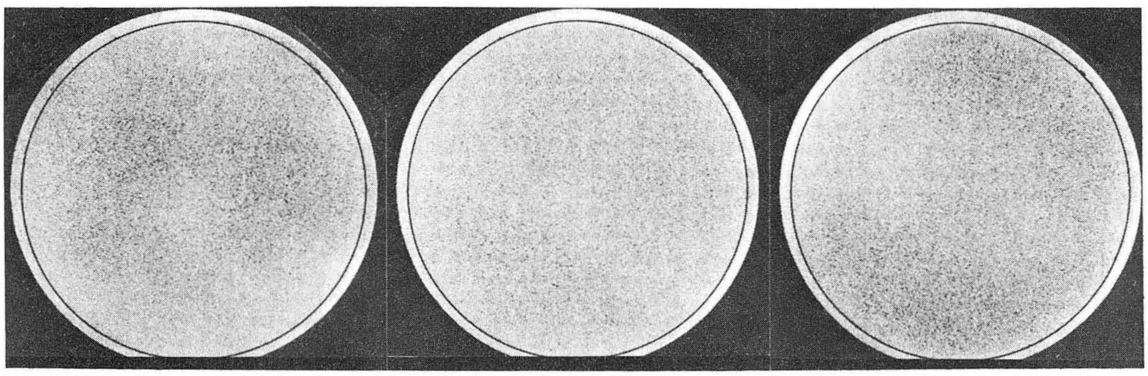

G. Flood with PHS window on lower portion of photopeak

H. Flood with PHS window centered

I. Flood with PHS window on upper portion of photopeak

Fig. 5 Nuclear-Chicago Pho/Gamma III HP at Sacramento Medical Center, Sacramento, California. Installed in 1968 and upgraded to HP status December, 1972.

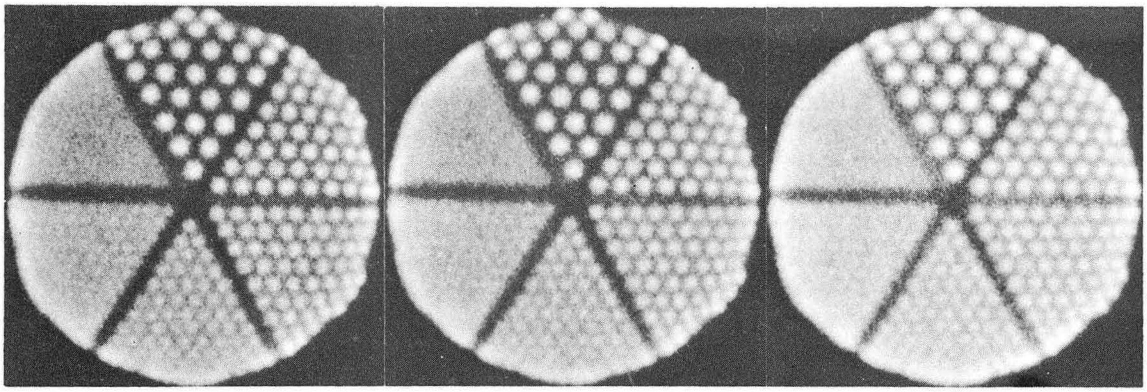

A. 0.76 mCi Equiv.
6,700 c/s
8,830 c/s/mCi

B. 1.9 mCi Equiv.
16,000 c/s
8,300 c/s/mCi

B. 4.9 mCi Equiv.
34,000 c/s
7,000 c/s/mCi

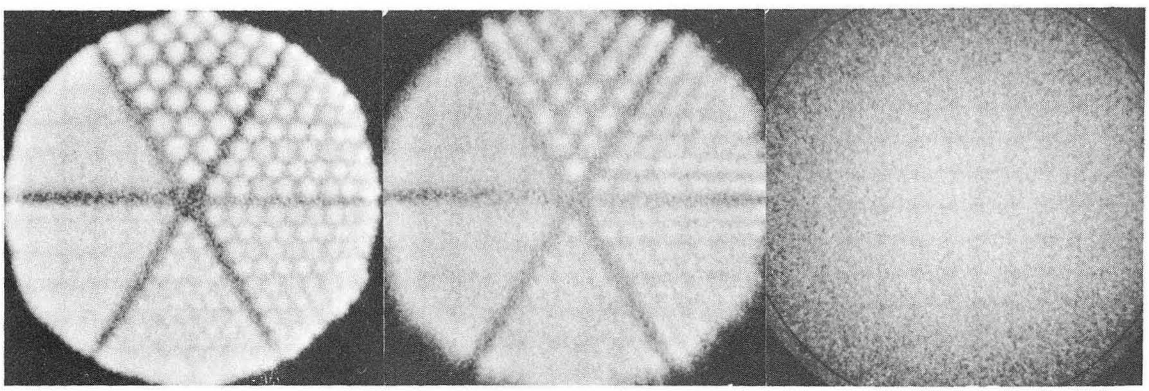

D. 12.5 mCi Equiv.
60,000 c/s
4,760 c/s/mCi

E. 32 mCi Equiv.
50,000 c/s
1,560 c/s/mCi

F. 80 mCi Equiv.
3,000 c/s
370 c/s/mCi

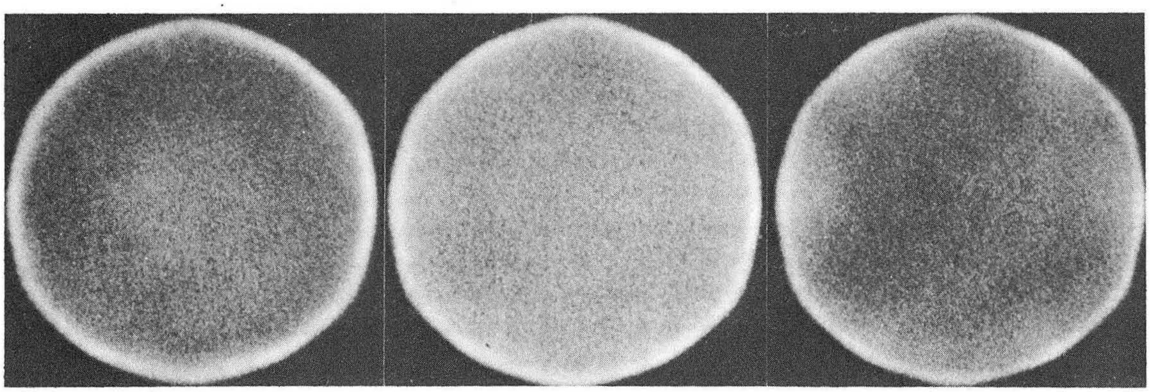

G. Flood with PHS window on lower portion of photopeak

H. Flood with PHS window centered on photopeak

I. Flood with PHS window on upper portion of photopeak

Fig. 6 Nuclear-Chicago Pho/Gamma III at Kaiser Hospital Oakland, California. Installed in 1968 and upgraded to HP status February, 1972.

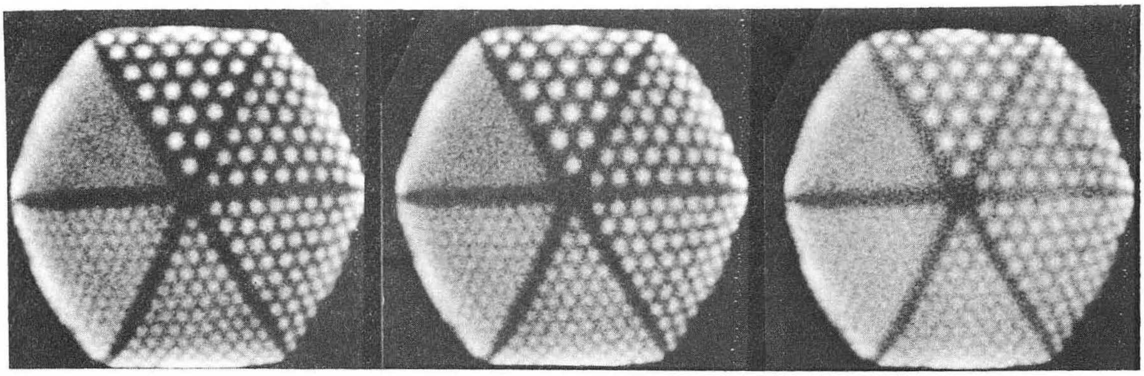

A. 0.84 mCi Equiv.
5,600 c/s
6,700 c/s/mCi

B. 2.1 mCi Equiv.
13,300 c/s
6,300 c/s/mCi

C. 5.4 mCi Equiv.
28,000 c/s
5,100 c/s/mCi

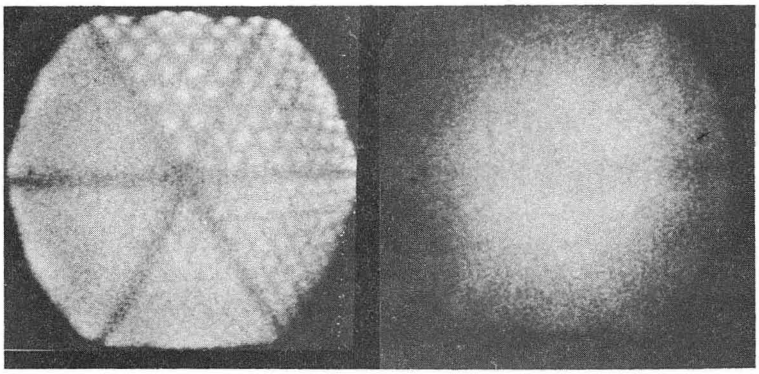

Note: This instrument is normally operated with the PHS window slightly below center to obtain better uniformity than is shown below.

D. 13.6 mCi Equiv.
43,500 c/s
3,200 c/s/mCi

E. 34 mCi Equiv.
29,400 c/s
865 c/s/mCi

F.

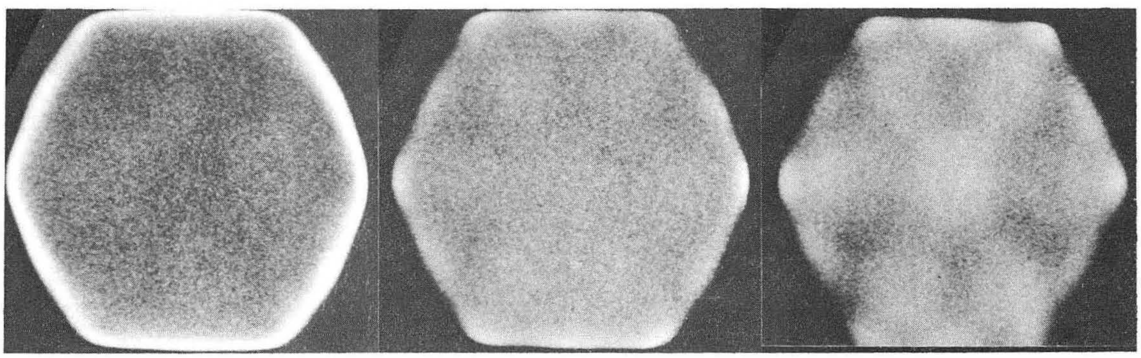

G. Flood with PHS window on lower portion of photopeak

H. Flood with PHS window centered on photopeak

I. Flood with PHS window on upper portion of photopeak

Fig. 7 Nuclear Data Radicamera installed April, 1973, at Herrick Hospital, Berkeley, California.

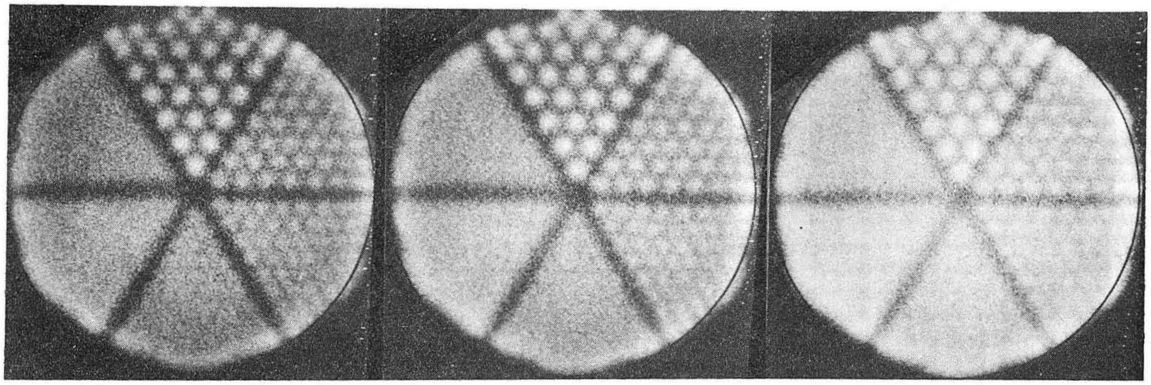

A. 0.9 mCi Equiv.
8,400 c/s
9,300 c/s/mCi

B. 2.3 mCi Equiv.
19,100 c/s
8,360 c/s/mCi

C. 5.8 mCi Equiv.
41,000 c/s
7,030 c/s/mCi

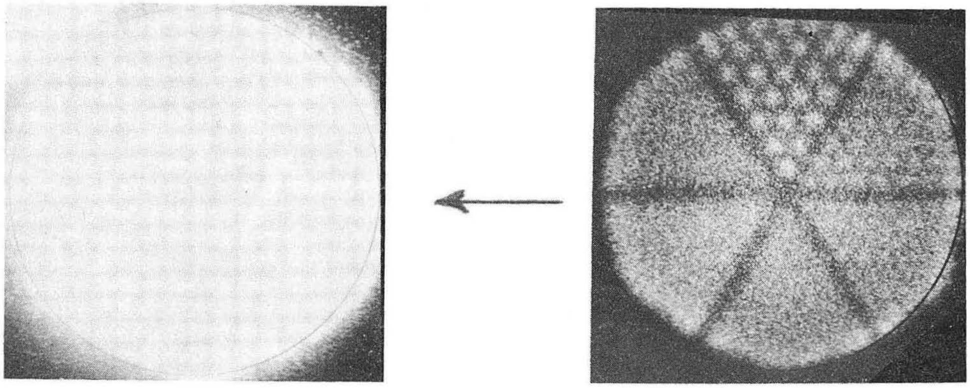

D. 15 mCi Equiv.
65,000 c/s
5,500 c/s/mCi

E. 15 mCi with CRT Intensity Reduced

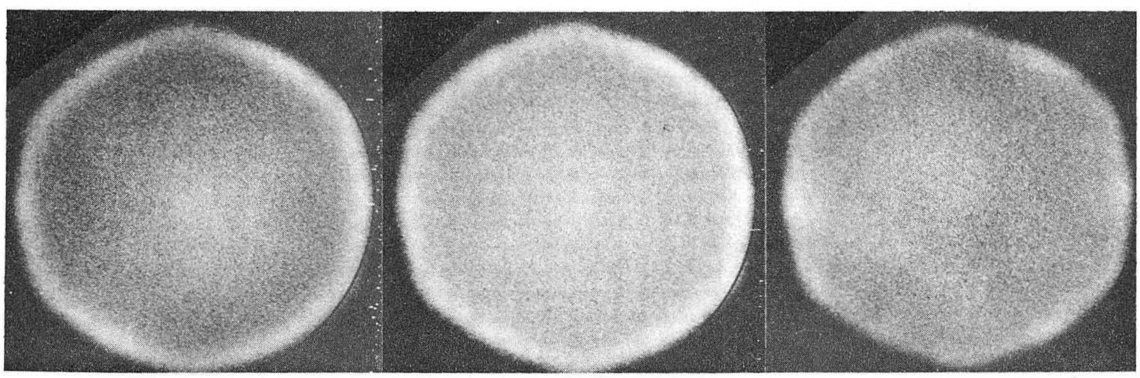

G. Flood with PHS window on lower portion of photopeak

H. Flood with PHS window centered on photopeak

I. Flood with PHS window on upper portion of photopeak

Fig. 8 Nuclear-Chicago Pho/Gamma III installed in 1966 at Ohio State University.

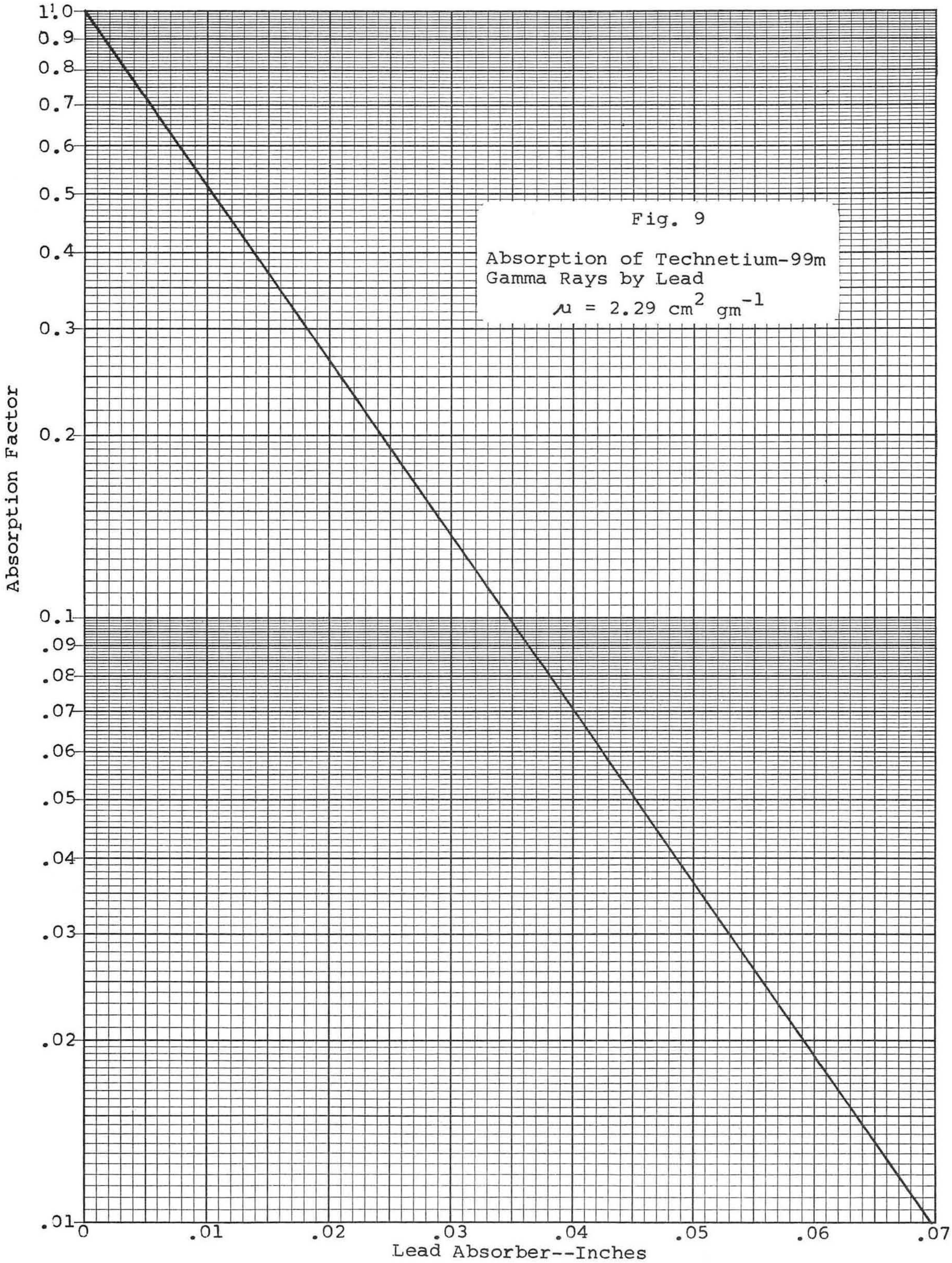

Fig. 9

Absorption of Technetium-99m Gamma Rays by Lead

$\mu = 2.29\ cm^2\ gm^{-1}$

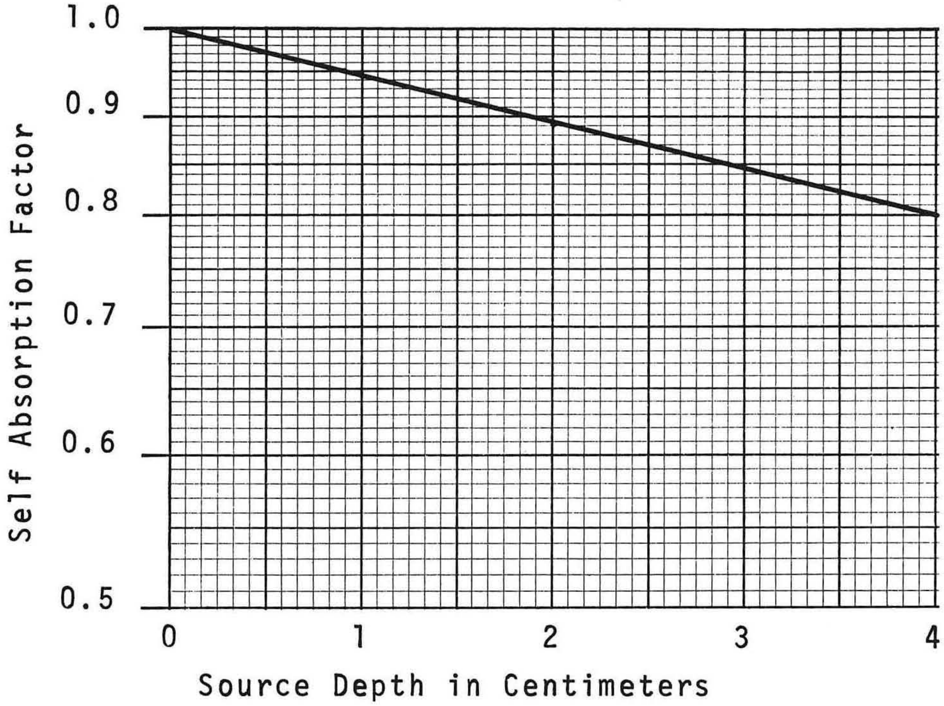

Fig. 10 Self absorption of Technetium-99m gamma rays in water, experimentally determined.